Electronic Supplementary Material (ESI) for Journal of Materials Chemistry A.

Mediator-free Z-scheme photocatalytic system based on ultrathin CdS nanosheets for efficient hydrogen evolution

Yi Huang,[a] Yang Liu,[b] Dongyang Zhu,[a] Yani Xin[a] and Bin Zhang*[a]

[a]Department of Chemistry, School of Science, Tianjin University, and Collaborative Innovation Centre of Chemical Science and Engineering (Tianjin), Tianjin 300072, China.

E-mail: bzhang@tju.edu.cn

[b]Analysis and testing center of Tianjin University, Tianjin University, Tianjin 300072, China.

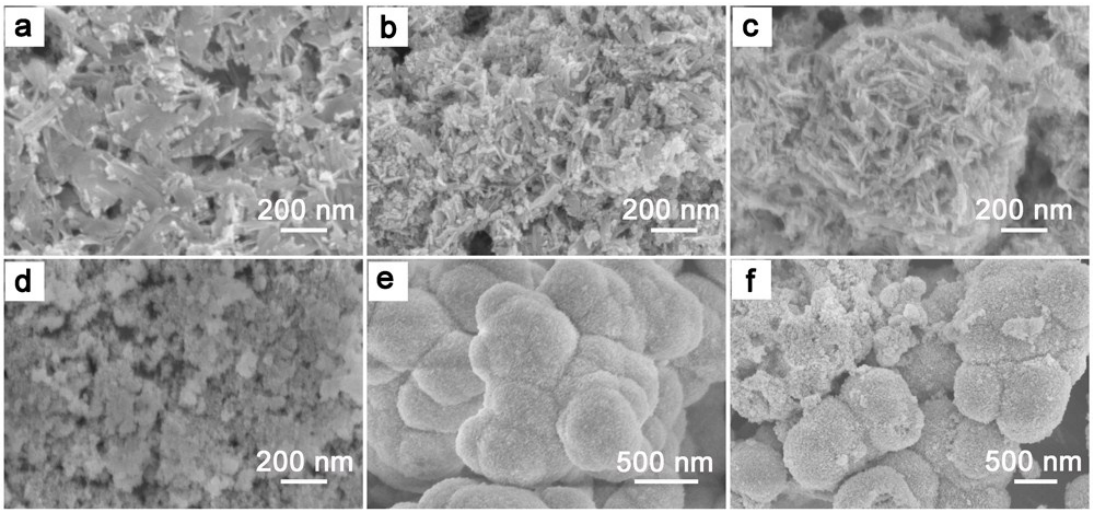

Figure S1 SEM images of the products prepared at 80 °C for 48 h with different volume ratio of V_{DETA}/V_{DIW}: (a) 12:0; (b) 4:1; (c) 2.5:1; (d) 1:1; (e) 1:2; (f) 1:4.

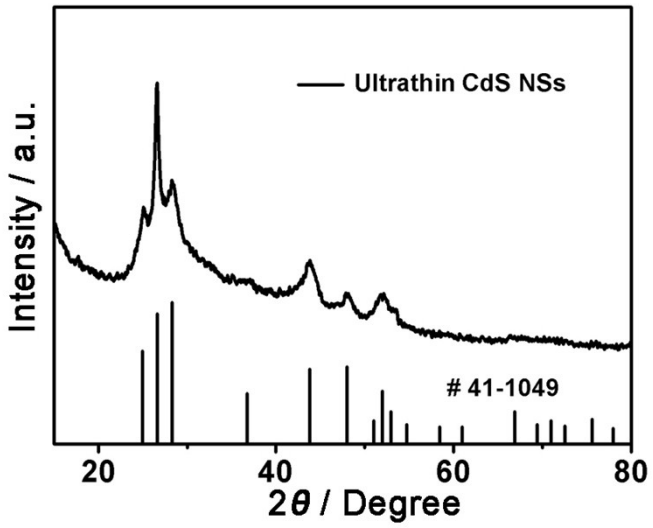

Figure S2 XRD spectra of ultrathin CdS NSs.

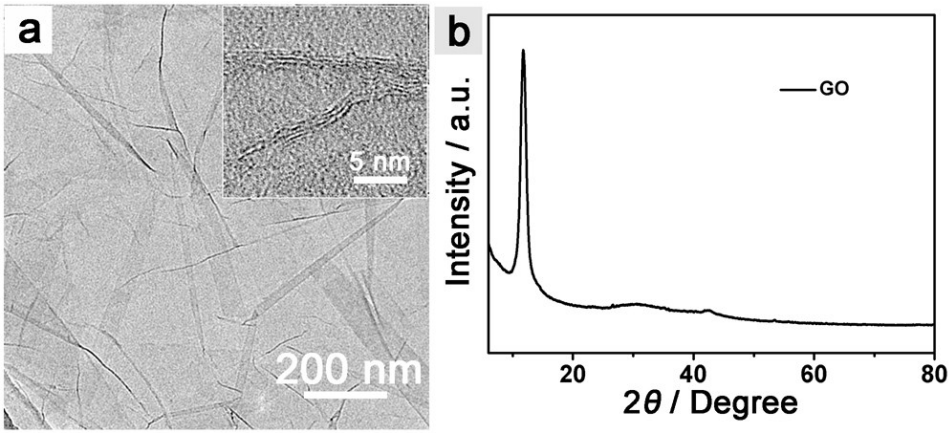

Figure S3 a) TEM image and b) XRD pattern of GO. The insert of a is HRTEM image of GO.

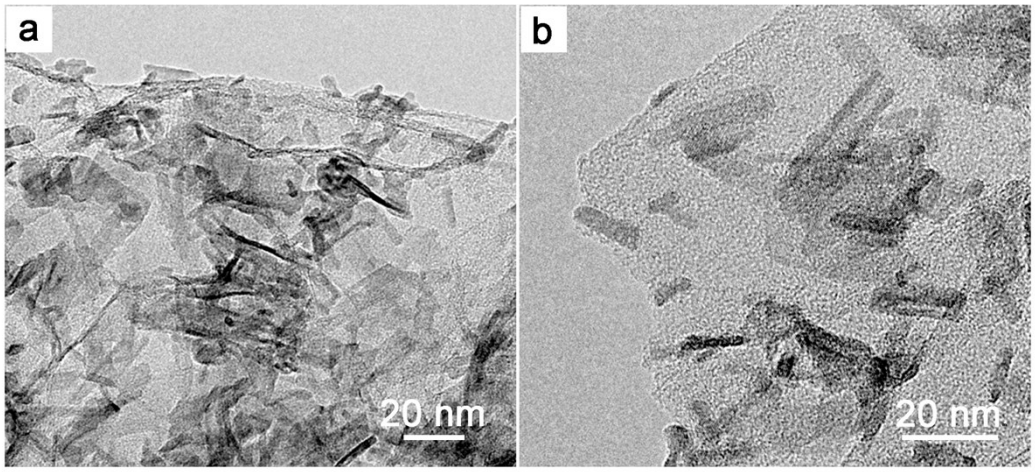

Figure S4 TEM images of CdS-NSs/RGO composite.

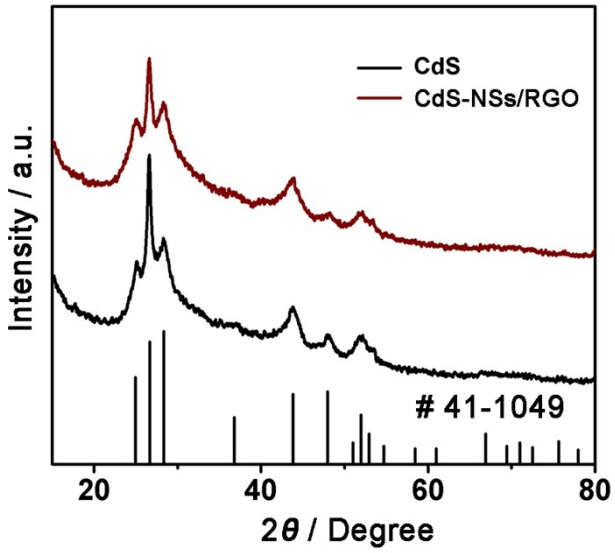

Figure S5 XRD spectra of ultrathin CdS NSs and CdS-NSs/RGO composite.

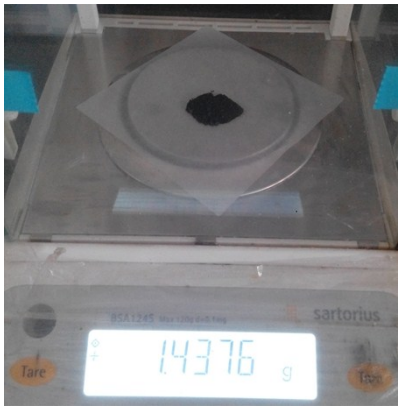

Figure S6 Photograph image of the CdS-NSs/RGO obtained in a large quantity of about 1.5 g.

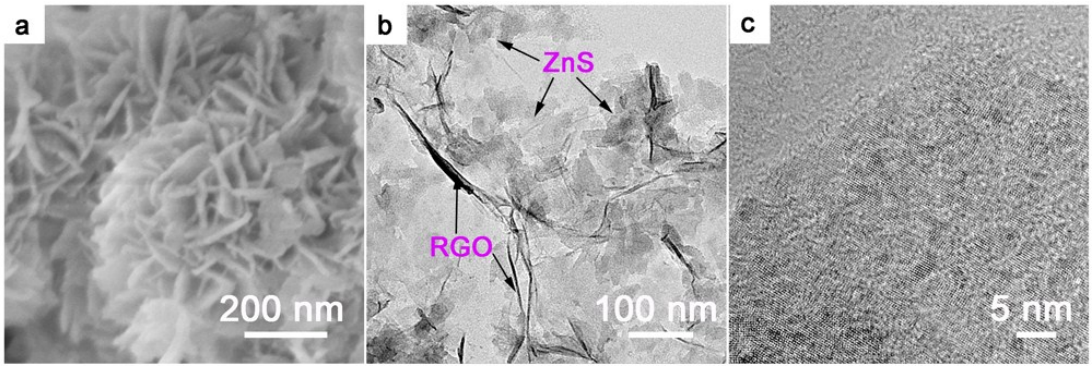

Figure S7 a) SEM image of ZnS NSs. b-c) TEM (b) and HRTEM (c) images of ZnS-NSs/RGO composites prepared by the same method depicted as the synthesis process of ultrathin CdS NSs and CdS-NSs/RGO.

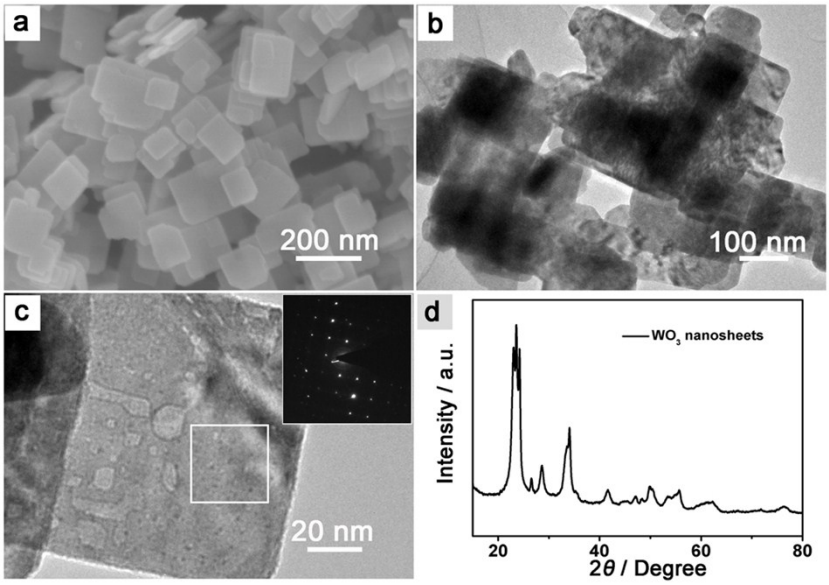

Figure S8 a) SEM image, b-c) TEM images and d) XRD pattern of the as-prepared WO_3 NSs. The insert of c is the selected-area electron diffraction (SAED) of the part of c (white square).

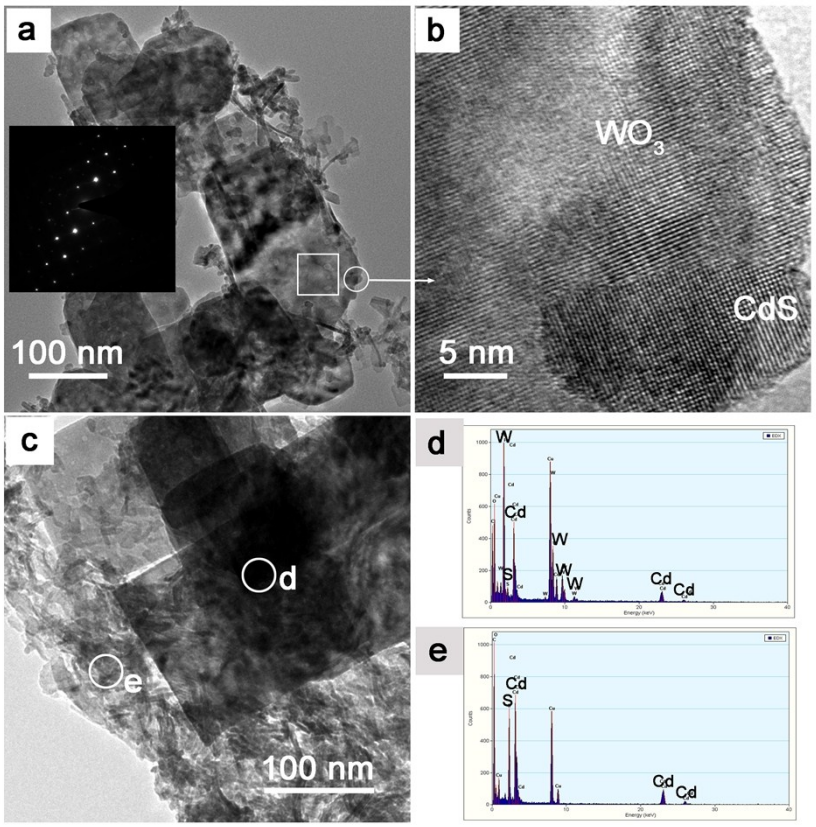

Figure S9 a) TEM image and b) HRTEM image of CdS-WO_3. The insert of a is the selected-area electron diffraction (SAED) of the part of a (white square). c) TEM image and EDS spectra of CdS/RGO-WO_3 composites. The d and e in c indicate the positions where the EDS spectra for (d) and (e) are collected. The CdS-WO_3 and CdS/RGO-WO_3 composites are obtained from the dispersion after the CdS NSs or CdS-NSs/RGO and WO_3 NSs sonic and stirring in an aqueous ethanol solution ($EtOH/H_2O$ = 1:1, v/v) at room temperature for 1 h. The TEM image in Fig. S8a shows the co-existence of the two kinds of nanosheets, big and small nanosheets. The SAED in the insert of a as same as the WO_3 NSs shown in the insert of Fig. S7c indicates the big NSs is WO_3 NSs. HRTEM image in Fig. S8b show that ultrathin CdS NSs can be combined well with WO_3 NSs. The EDS spectra of CdS/RGO-WO_3 composites (Fig. S8d,e) obtained from the Fig S8c also show that the co-existence of the ultrathin CdS NSs and WO_3 NSs.

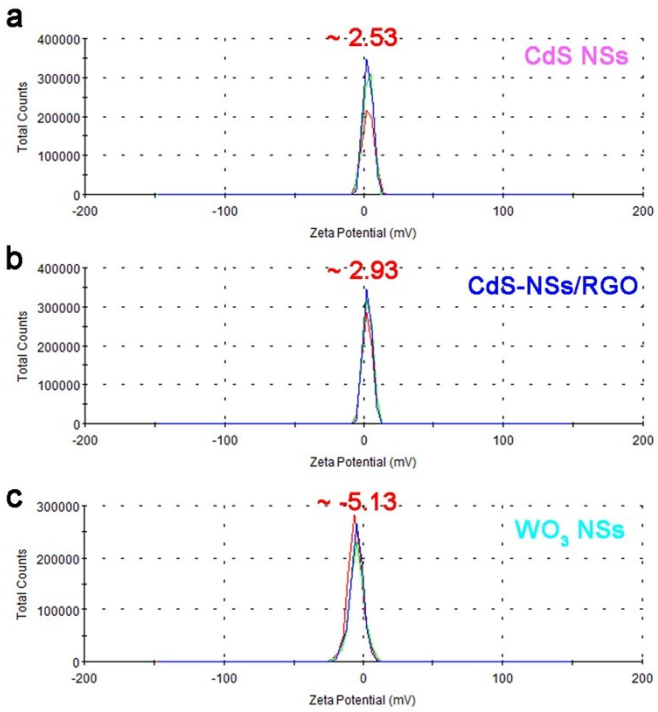

Figure S10 Zeta potential test of a) CdS NSs, b) CdS-NSs/RGO composites and WO_3 NSs dispersion in an aqueous ethanol solution ($EtOH/H_2O$ = 1:1, v/v) at room temperature. The samples were measured for three times. It was found that the zeta potential of three samples were about +2.53 mV, +2.93 mV and -5.13 mV, respectively.

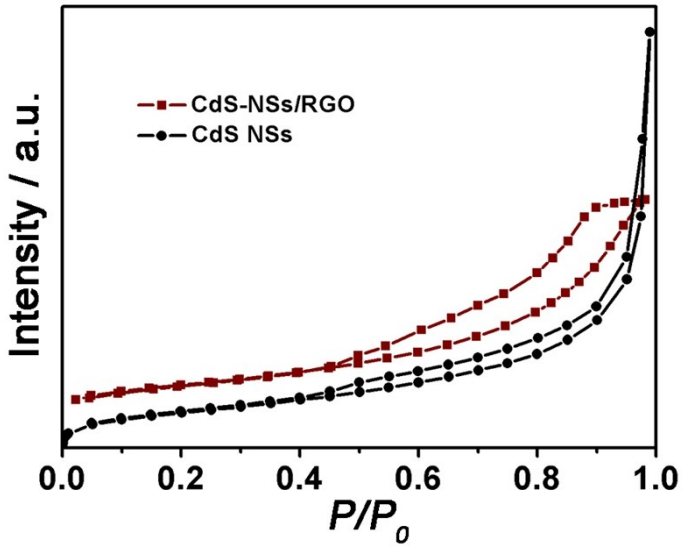

Figure S11 Nitrogen adsorption/desorption isotherms of CdS NSs and CdS-NSs/RGO composites. Brunauer-Emmett-Teller (BET) surface area of CdS NSs and CdS-NSs/RGO composites are determined to be 87.0 m^2/g and 137.9 m^2/g, respectively.

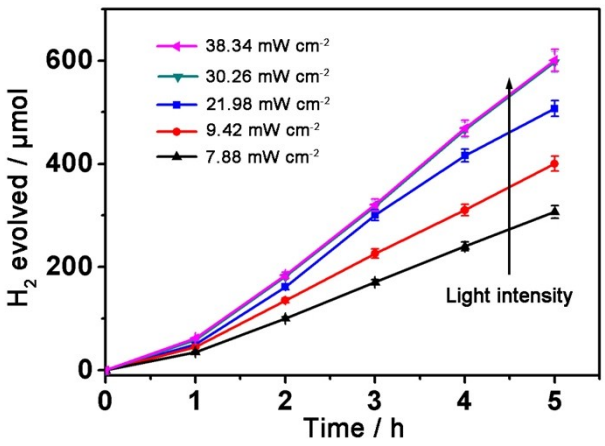

Figure S12 Photocatalytic hydrogen production from system containing CdS-NSs/RGO (12mg), WO_3 NSs (2 mg) in an aqueous ethanol solution ($EtOH/H_2O$ = 1:1, v/v) at room temperature upon irradiation with 420 nm band-pass filters when light intensity was 7.88 mW cm^{-2} (black), 9.42 mW cm^{-2} (red), 21.98 mW cm^{-2} (blue), 30.26 mW cm^{-2} (green), 38.34 mW cm^{-2} (pink).

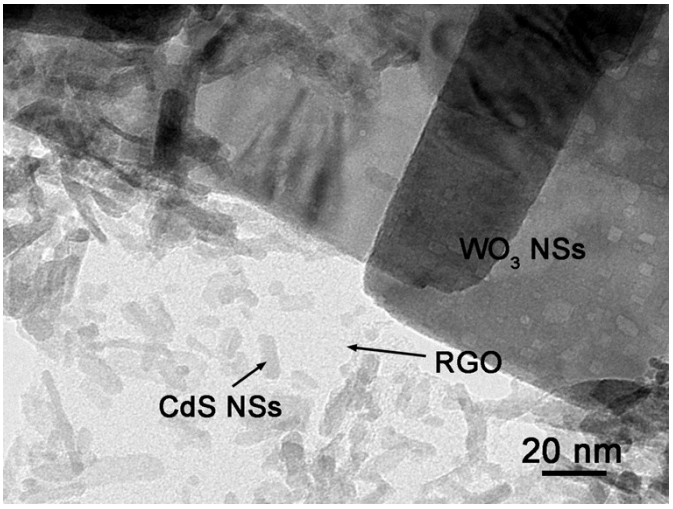

Figure S13 TEM image of CdS/RGO-WO_3 composite photocatalytic system after visible-light irradiation for 36 h.

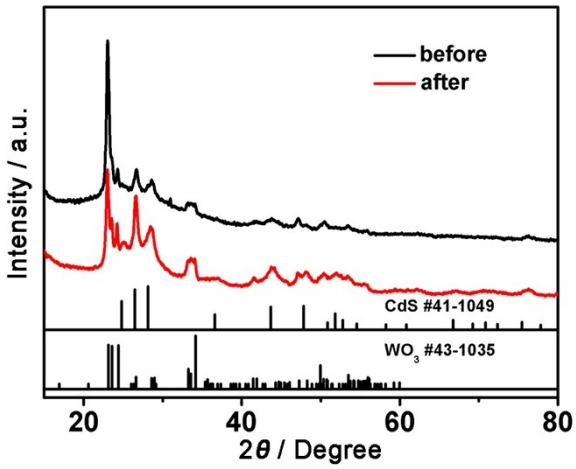

Figure S14 XRD patterns of CdS/RGO-WO_3 composite photocatalytic system before and after visible-light irradiation for 36 h.

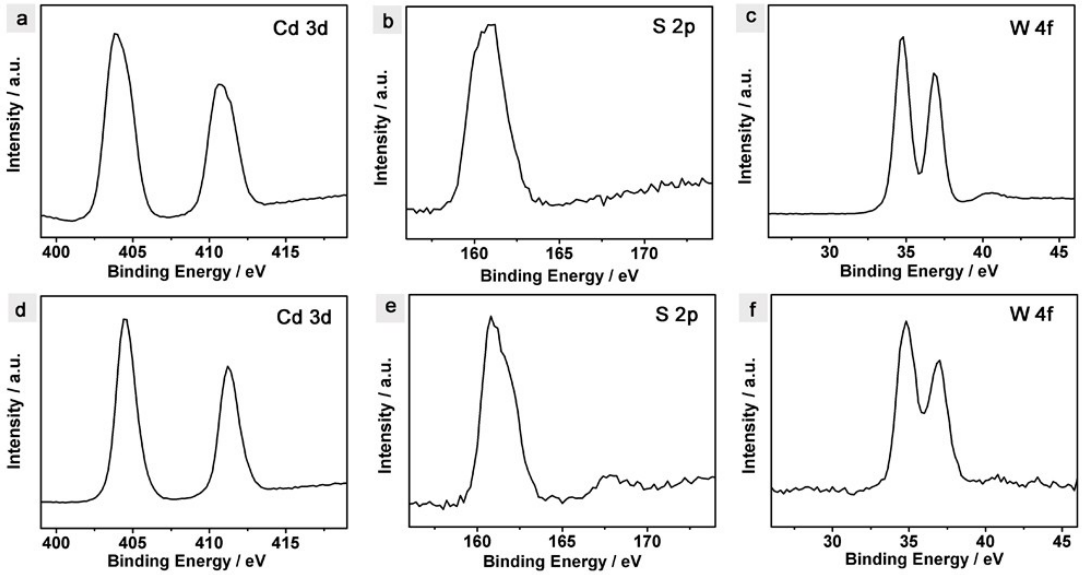

Figure S15 XPS spectra of CdS/RGO-WO_3 (12 mg CdS-NSs/RGO and 2 mg WO_3 NSs) before (a-c) and after (d-f) visible-light irradiation for 36 h. (a, d) Cd3d spectrum. (b, e) S2p spectrum. (c, f) W4f spectrum.

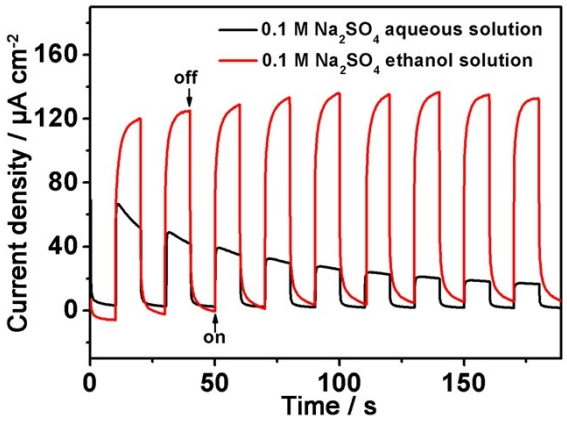

Figure S16 The comparison of transient photocurrent responses of the CdS/RGO-WO_3 composite photocatalytic system at 0.6 V *vs*. SCE with on/off cycles under visible light illumination ($\lambda > 420$ nm) in the presence of 0.1 M Na_2SO_4 aqueous solution and ethanol solution (10 %, v/v) as electrolyte.

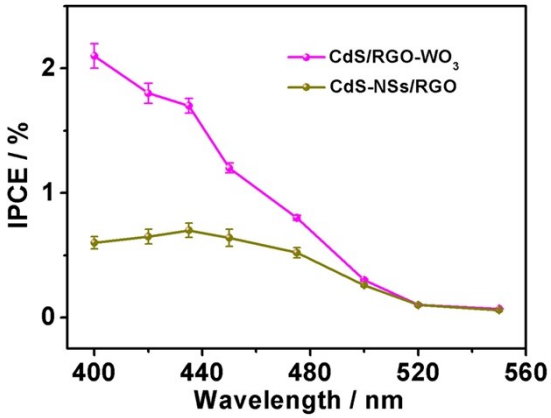

Figure S17 The IPCE spectra of CdS-NSs/RGO and CdS/RGO-WO_3 in 0.5 M Na_2SO_4 measured at 0.6 V vs. SCE.

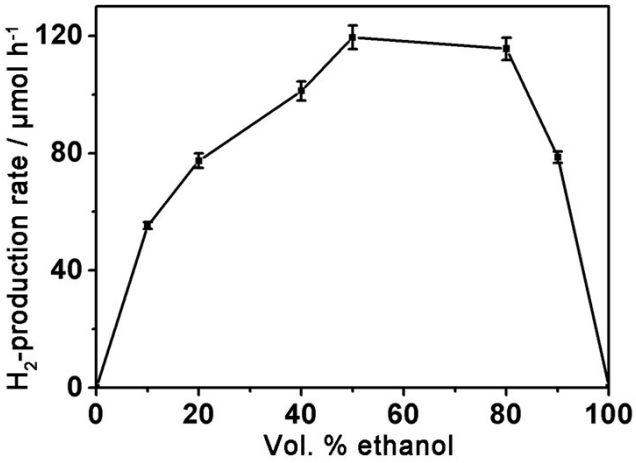

Figure S18 H_2-production rate versus ethanol concentration in the presence of 12 mg CdS-NSs/RGO and 2 mg WO_3 NSs at room temperature under irradiation of visible light.

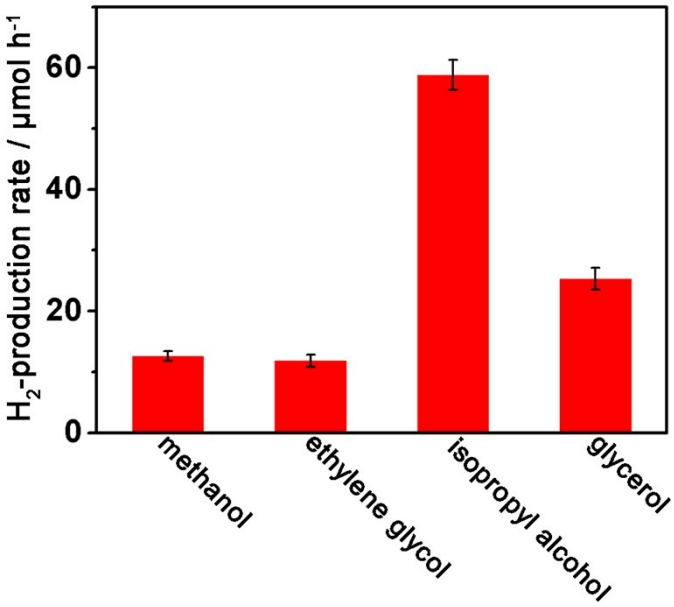

Figure S19 Photocatalytic H_2 production from system containing CdS-NSs/RGO (12mg), WO_3 NSs (2 mg) in different alcohol aqueous (1:1, v/v) at room temperature upon under irradiation of visible light.

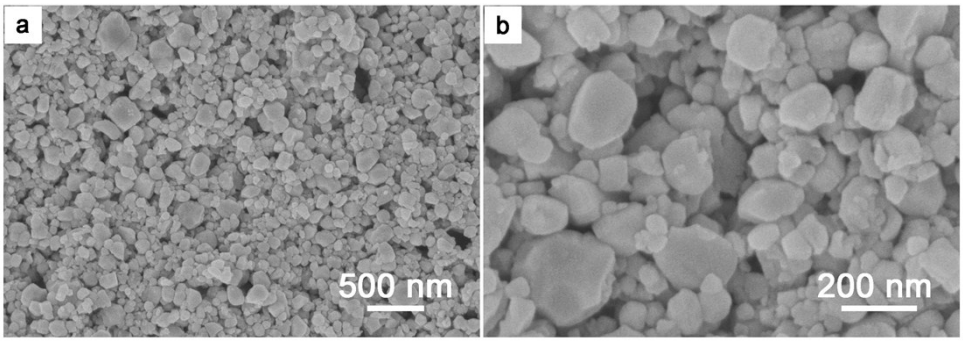

Figure S20 SEM images of commercial WO_3 nanoparticles (WO_3 NPs).

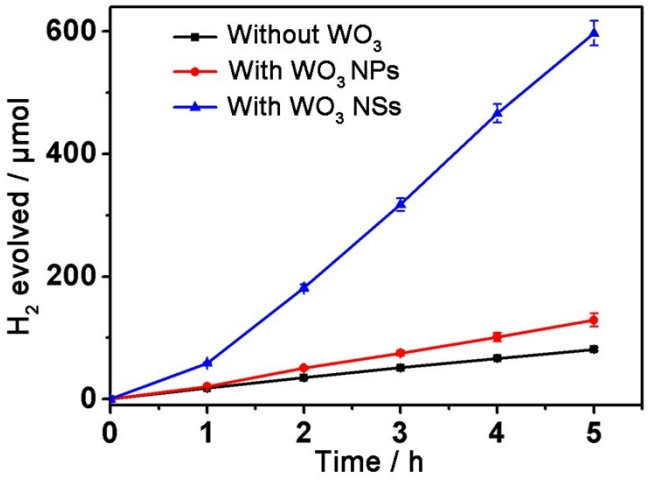

Figure S21 Time-dependent H_2 evolution under visible-light irradiation of the CdS-NSs/RGO (12 mg) without WO_3 NSs (black line) and with commercial WO_3 nanoparticles (WO_3 NPs, red line) and WO_3 NSs (blue line).

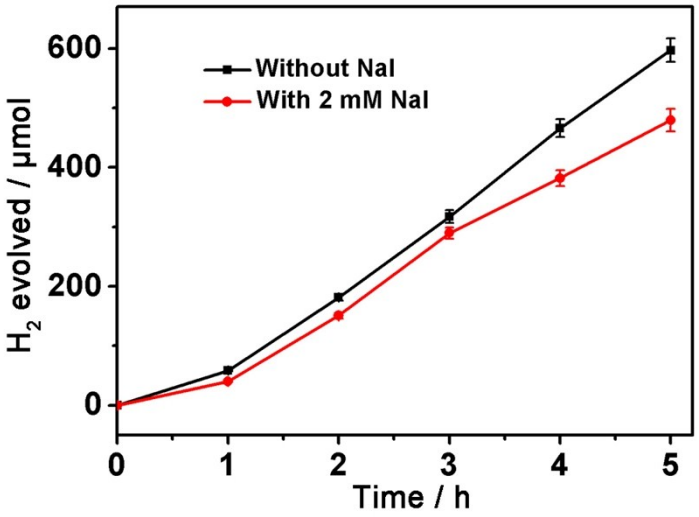

Figure S22 Time-dependent H_2 evolution from system containing CdS-NSs/RGO (12mg), WO_3 NSs (2 mg) in 30 mL ethanol solution ($EtOH/H_2O$ = 1:1, v/v) with or without NaI (15 mg) at room temperature upon under irradiation of visible light. As shown in this figure, the activity of photocatalytic hydrogen evolution is less decrease when NaI is added into the Z-scheme photocatalytic system as redox mediator, which may be attributed to the backward reactions over the two semiconductors of Z-scheme photocatalytic system.[1-3]

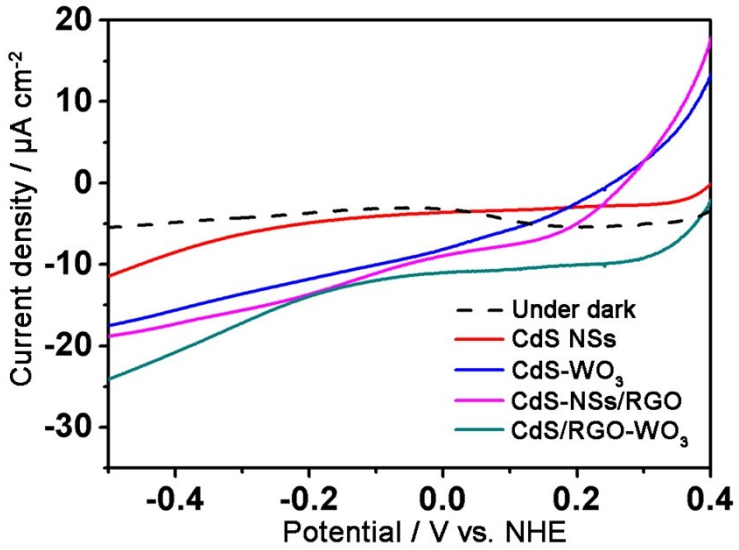

Figure S23 Current-potential curves of the CdS NSs, CdS-WO_3, CdS-NSs/RGO and CdS/RGO-WO_3 combined with NiO as photocathode obtained in the dark and under visible light irradiation by taking the sample photoelectrode (1.0 cm^2) as working electrode, SCE as reference electrode, platinum sheet as counter electrode, and 0.1 M Na_2SO_4 as electrolyte under 300 W Xe lamp illumination with a UV filter.

Table S1 Summary of the amount of H_2 production and AQE after irradiation for 5 h under different light intensity.

Light intensity / mW cm^{-2}	Amount of H_2 production after irradiation for 5 h[a]	AQE / %[a]
7.88	306.8	9.8
9.42	400.1	10.7
21.98	507	5.8
30.26	597	5.0
38.34	600.7	3.9

[a] The values are average from three independent experiments.

Table S2 Comparison of photocatalytic H_2 production characteristics with other similar photocatalysts.

System	**Photocatalyst mass (mg)**	**Sacrificial reagents**	**H_2 rate (μmol h^{-1})**	**Stability(h)**	**Ref.**
CdS-WO_3	**14**	**ethanol**	**32.65±2.1**	**-**	**This work**
CdS/RGO-WO_3	**14**	**ethanol**	**119.4 ± 4.0**	**36**	**This work**
CNDs/WO_3	48	methanol	16.49	40	[4]
g-CNS/Au/CdS	100	lactic acid	88.3	25	[5]
CdS/WO_3	50	lactic acid	18.45	9	[6]
$W_{18}O_{49}$/g-C_3N_4	5	TEA	3.69	6	[7]
CdS/Au/ZnO	100	Na_2SO_3 + Na_2S	60.8	10	[8]

Reference

1. P. Zhou, J. Yu and M. Jaroniec, *Adv. Mater.*, 2014, **26**, 4920-4935.
2. H. Li, W. Tu, Y. Zhou and Z. Zou, *Adv. Sci.*, 2016, DOI: 10.1002/advs.201500389.
3. K. Sayama, K. Mukasa, R. Abe, Y. Abe and H. Arakawa, *Chem. Commun.*, 2001, **23**, 2416-2417.
4. P. Yang, J. Zhao, J. Wang, B. Cao, L. Li and Z. Zhu, *J. Mater. Chem. A*, 2015, **3**, 8256-8259.
5. W. Li, C. Feng, S. Dai, J. Yue, F. Hua and H. Hou, *Appl. Catal. B-Environ.*, 2015, **168-169**, 465-471.
6. L. J. Zhang, S. Li, B. K. Liu, D. J. Wang and T. F. Xie, *ACS Catal.*, 2014, **4**, 3724-3729.
7. K. Song, F. Xiao, L. Zhang, F. Yue, X. Liang, J. Wang and X. Su, *J. Mol. Catal. A-Chem.*, 2016, **418-419**, 95-102.
8. Z. B. Yu, Y. P. Xie, G. Liu, G. Q. Lu, X. L. Ma and H.-M. Cheng, *J. Mater. Chem. A*, 2013, **1**, 2773.